

AN AXIAL CRACK IN A PRESSURIZED CYLINDRICAL SHELL

E. S. Folias*

ABSTRACT

Following an earlier analysis of a line crack in a spherical cap, the stresses in a cylindrical shell containing an axial crack are presented. The inverse square root singular behavior of the stresses peculiar to crack problems is obtained in both the extensional and bending components. This singularity may be related to that found in an initially flat plate by

$$\frac{\sigma_{\text{shell}}}{\sigma_{\text{plate}}} \approx 1 + (a + b \ln \frac{c}{\sqrt{Rh}}) \frac{c^2}{Rh} + \dots$$

where the quantity in parentheses is positive. An approximate fracture criterion, based on Griffith's Theory, is also deduced, and bending-stretching interaction curves for this case are presented.

INTRODUCTION

In a recent paper⁽¹⁾, the stress fields in the vicinity of a line crack in a spherical cap were determined. It was pointed out that bending loads induce extensional stresses, and vice versa, so that the subject of eventual concern is the simultaneous stress fields produced in an initially curved sheet containing a crack. Of the two simple geometries which may first come to mind, a spherical shell, and a cylindrical shell, the former was studied first because the radius of curvature is constant in all directions, affording considerable mathematical simplification. In the latter case, however, the radius varies between a constant and infinity as one considers different angular positions with respect to the point of a crack aligned parallel to the cylinder axis. In a previous treatment of this problem, Sechler and Williams⁽²⁾ suggested an approximate equation based upon the behavior of a beam on an elastic foundation, and were able to obtain reasonable agreement with experimental results. Using techniques developed earlier, the author has been able to investigate this problem analytically, and the results are given below; certain details of this work have been omitted here but may be found elsewhere⁽³⁾.

FORMULATION OF THE PROBLEM

Consider a portion of a thin, shallow cylindrical shell of constant thickness h and subjected to an internal pressure q_0 . The material of the shell is assumed to be homogeneous and isotropic; parallel to the axis there exists a cut of length $2c$. Following Marguerre⁽⁴⁾, the coupled differential equations governing the displacement function W and the stress function F , with x and y as dimensionless rectangular coordinates of the base plane (see Figure 1) are given by

$$\frac{E h c^2}{R} \frac{\partial^2 W}{\partial x^2} + \nabla^4 F = 0 \quad (1)$$

$$\nabla^4 W - \frac{c^2}{R D} \frac{\partial^2 F}{\partial x^2} = \frac{q_0}{D} c^4 \quad (2)$$

* Formerly Research Fellow at the California Institute of Technology. Dr. Folias is currently in Thessaloniki, Greece; mailing address is c/o the editorial office, Pasadena, California.

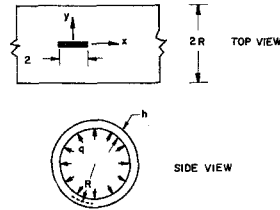


Figure 1. Geometry and Coordinates

where R is the radius of the cylinder. As to boundary conditions, one must require that the normal moment, equivalent vertical shear, and normal and tangential in-plane stresses vanish along the crack. However, suppose that one has already found* a particular solution satisfying eqns 1 and 2, but that there is a residual normal moment M_y , equivalent vertical shear V_y , normal in-plane stress N_y , and in-plane tangential stress N_{xy} , along the crack $|x| < 1$ of the form:

$$M_y^{(P)} = - D m_0 / c^2 \quad (3)$$

$$V_y^{(P)} = 0 \quad (4)$$

$$N_y^{(P)} = - n_0 / c^2 \quad (5)$$

$$N_{xy}^{(P)} = 0 \quad (6)$$

where m_0 and n_0 will be considered constants for simplicity.

Assuming, therefore, that a particular solution has been found, we need to find two functions of the dimensionless coordinates (x, y) , $W(x, y)$ and $F(x, y)$, such that they satisfy the partial differential equations 1 and 2 and the following boundary conditions.

At $y = 0$ and $|x| < 1$:

$$M_y(x, 0) = - \frac{D}{c^2} \left[\frac{\partial^2 W}{\partial y^2} + \nu \frac{\partial^2 W}{\partial x^2} \right] = \frac{D m_0}{c^2} \quad (7)$$

$$V_y(x, 0) = - \frac{D}{c^3} \left[\frac{\partial^3 W}{\partial y^3} + (2 - \nu) \frac{\partial^3 W}{\partial x^2 \partial y} \right] = 0 \quad (8)$$

$$N_y(x, 0) = \frac{1}{c^2} \frac{\partial^2 F}{\partial x^2} = \frac{n_0}{c^2} \quad (9)$$

$$N_{xy}(x, 0) = - \frac{1}{c^2} \frac{\partial^2 F}{\partial x \partial y} = 0 \quad (10)$$

At $y = 0$ and $|x| > 1$ we must satisfy the continuity requirements, namely

* As an illustration of how the local solution may be combined in a particular case see Reference 3.

$$\lim_{|y| \rightarrow 0} \left[\frac{\partial^n}{\partial y^n} (W^+) - \frac{\partial^n}{\partial y^n} (W^-) \right] = 0 \quad (11)$$

$$\lim_{|y| \rightarrow 0} \left[\frac{\partial^n}{\partial y^n} (F^+) - \frac{\partial^n}{\partial y^n} (F^-) \right] = 0 \quad (12)$$

$$n = 0, 1, 2, 3.$$

Furthermore, we shall limit ourselves to large radii of curvature, i.e., small deviations from flat sheets; we thus require that the displacement function W and the stress function F together with their first derivatives be finite far from the crack. In this manner, we avoid infinite stresses and displacements in the region far away from the crack. These restrictions at infinity simplify the mathematical complexities of the problem considerably, and correspond to the usual expectations of St. Venant's principle.

METHOD OF SOLUTION

We construct the following integral representations which have the proper symmetrical behavior with respect to x , with $\lambda^4 = Ehc^4/R^2D$

$$W(x, y^\pm) = \int_0^\infty \left\{ P_1 e^{-\sqrt{s(s-\lambda\alpha)}|y|} + P_2 e^{-\sqrt{s(s+\lambda\alpha)}|y|} + P_3 e^{-\sqrt{s(s-\lambda\beta)}|y|} + P_4 e^{-\sqrt{s(s+\lambda\beta)}|y|} \right\} \cos xs \, ds \quad (13)$$

$$F(x, y^\pm) = -i\sqrt{EhD} \int_0^\infty \left\{ P_1 e^{-\sqrt{s(s-\lambda\alpha)}|y|} + P_2 e^{-\sqrt{s(s+\lambda\alpha)}|y|} - P_3 e^{-\sqrt{s(s-\lambda\beta)}|y|} - P_4 e^{-\sqrt{s(s+\lambda\beta)}|y|} \right\} \cos xs \, ds \quad (14)$$

where the P_i ($i = 1, 2, 3, 4$) are arbitrary functions of s to be determined from the boundary conditions, and the \pm signs refer to $y > 0$ and $y < 0$, respectively. Also $\alpha = i^{\frac{1}{2}}$, $\beta = (-i)^{\frac{1}{2}}$.

Assuming that we can differentiate under the integral sign, formally substituting eqns 13 and 14 into eqns 7-10 yields respectively:

$$\lim_{|y| \rightarrow 0} \int_0^\infty - \left\{ P_1 s (v_0 s - \lambda\alpha) e^{-\sqrt{s(s-\lambda\alpha)}|y|} + P_2 s (v_0 s + \lambda\alpha) e^{-\sqrt{s(s+\lambda\alpha)}|y|} + P_3 s (v_0 s - \lambda\beta) e^{-\sqrt{s(s-\lambda\beta)}|y|} + P_4 s (v_0 s + \lambda\beta) e^{-\sqrt{s(s+\lambda\beta)}|y|} \right\} \cos xs \, ds = m_0; \quad (15)$$

$$|x| < 1$$

$$\lim_{|y| \rightarrow 0} \pm \int_0^\infty \left\{ P_1 s (v_0 s + \lambda\alpha) \sqrt{s(s-\lambda\alpha)} e^{-\sqrt{s(s-\lambda\alpha)}|y|} + P_2 s (v_0 s - \lambda\alpha) \sqrt{s(s+\lambda\alpha)} e^{-\sqrt{s(s+\lambda\alpha)}|y|} + P_3 s (v_0 s + \lambda\beta) \sqrt{s(s-\lambda\beta)} e^{-\sqrt{s(s-\lambda\beta)}|y|} + P_4 s (v_0 s - \lambda\beta) \sqrt{s(s+\lambda\beta)} e^{-\sqrt{s(s+\lambda\beta)}|y|} \right\} \cos xs \, ds = 0; \quad (16)$$

$$|x| < 1$$

$$\pm \lim_{|y| \rightarrow 0} i \sqrt{E h D} \int_0^{\infty} \left\{ P_1 e^{-\sqrt{s(s-\lambda\alpha)} |y|} + P_2 e^{-\sqrt{s(s+\lambda\alpha)} |y|} - P_3 e^{-\sqrt{s(s-\lambda\beta)} |y|} - P_4 e^{-\sqrt{s(s+\lambda\beta)} |y|} \right\} s^2 \cos xs \, ds = n_0; \quad (17)$$

$|x| < 1$

$$\lim_{|y| \rightarrow 0} i \sqrt{E h D} \int_0^{\infty} \left\{ P_1 \sqrt{s(s-\lambda\alpha)} e^{-\sqrt{s(s-\lambda\alpha)} |y|} + P_2 \sqrt{s(s+\lambda\alpha)} e^{-\sqrt{s(s+\lambda\alpha)} |y|} - P_3 \sqrt{s(s-\lambda\beta)} e^{-\sqrt{s(s-\lambda\beta)} |y|} - P_4 \sqrt{s(s+\lambda\beta)} e^{-\sqrt{s(s+\lambda\beta)} |y|} \right\} s \sin xs \, ds = 0; \quad (18)$$

$|x| < 1$

where again the \pm signs refer to $y > 0$ and $y < 0$, respectively, and $v_0 = 1 - v$. A sufficient condition for 16 and 18 to be satisfied is to set the integrands equal to zero. This leads to:

$$\begin{aligned} \sqrt{s(s-\lambda\beta)} P_3 &= - \left(\frac{v_0 s}{\lambda\beta} - \frac{1}{2} \right) \left[\sqrt{s(s-\lambda\alpha)} P_1 + \sqrt{s(s+\lambda\alpha)} P_2 \right] \\ &\quad - \frac{\alpha}{2\beta} \left[\sqrt{s(s-\lambda\alpha)} P_1 - \sqrt{s(s+\lambda\alpha)} P_2 \right] \end{aligned} \quad (19)$$

$$\begin{aligned} \sqrt{s(s+\lambda\beta)} P_4 &= \left(\frac{v_0 s}{\lambda\beta} + \frac{1}{2} \right) \left[\sqrt{s(s-\lambda\alpha)} P_1 + \sqrt{s(s+\lambda\alpha)} P_2 \right] \\ &\quad + \frac{\alpha}{2\beta} \left[\sqrt{s(s-\lambda\alpha)} P_1 - \sqrt{s(s+\lambda\alpha)} P_2 \right] \end{aligned} \quad (20)$$

Next, it may easily be shown that the continuity conditions are satisfied if we consider the following combinations to vanish

$$\int_0^{\infty} \left\{ P_1 \sqrt{s(s-\lambda\alpha)} \left(1 + \frac{\lambda\alpha}{s} \right) + P_2 \sqrt{s(s+\lambda\alpha)} \left(1 - \frac{\lambda\alpha}{s} \right) \right\} \cos xs \, ds = 0; \quad |x| > 1 \quad (21)$$

$$\int_0^{\infty} \left\{ P_1 \sqrt{s(s-\lambda\alpha)} \left(1 - \frac{\lambda\alpha}{s} \right) + P_2 \sqrt{s(s+\lambda\alpha)} \left(1 + \frac{\lambda\alpha}{s} \right) \right\} \cos xs \, ds = 0; \quad |x| > 1 \quad (22)$$

We have thus reduced our problem to solving the dual integral equations 15, 17, 21, and 22 for the unknown functions $P_1(s)$ and $P_2(s)$. These may be transformed to a set of coupled singular integral equations of the Cauchy type, a solution of which may be found in a series form for small values of the parameter λ . Details of the method of solution may be found in Reference 3. It is an easy matter to show that the physical range of λ is $0 \leq \lambda < 20$ and for most practical cases $0 \leq \lambda < 2$, depending upon the size of the crack.

Without going into the details, the displacement and stress functions are:

$$\begin{aligned}
W(x, y^{\pm}) = & \int_0^{\infty} \left\{ \left(\frac{A_0}{s} + \frac{B_0}{\lambda\alpha} \right) \frac{J_1(s)}{2\sqrt{s(s-\lambda\alpha)}} e^{-\sqrt{s(s-\lambda\alpha)}|y|} \right. \\
& + \left. \left(\frac{A_0}{s} - \frac{B_0}{\lambda\alpha} \right) \frac{J_1(s)}{2\sqrt{s(s+\lambda\alpha)}} e^{-\sqrt{s(s+\lambda\alpha)}|y|} - \left[\frac{v_0 s}{\lambda\beta} - \frac{1}{2} \frac{A_0}{s} + \frac{B_0}{2\lambda\beta} \right] \right. \\
& \frac{J_1(s)}{\sqrt{s(s-\lambda\beta)}} e^{-\sqrt{s(s-\lambda\beta)}|y|} + \left. \left[\frac{v_0 s}{\lambda\beta} + \frac{1}{2} \frac{A_0}{s} + \frac{B_0}{2\lambda\beta} \right] \right. \\
& \left. \frac{J_1(s)}{\sqrt{s(s+\lambda\beta)}} e^{-\sqrt{s(s+\lambda\beta)}|y|} + \dots \right\} \cos xs ds
\end{aligned} \tag{23}$$

$$\begin{aligned}
F(x, y^{\pm}) = & -i\sqrt{EhD} \int_0^{\infty} \left\{ \left(\frac{A_0}{s} + \frac{B_0}{\lambda\alpha} \right) \frac{J_1(s) e^{-\sqrt{s(s-\lambda\alpha)}|y|}}{2\sqrt{s(s-\lambda\alpha)}} + \left(\frac{A_0}{s} - \frac{B_0}{\lambda\alpha} \right) \right. \\
& \frac{J_1(s) e^{-\sqrt{s(s+\lambda\alpha)}|y|}}{2\sqrt{s(s+\lambda\alpha)}} + \left. \left[\frac{v_0 s}{\lambda\beta} - \frac{1}{2} \frac{A_0}{s} + \frac{B_0}{2\lambda\beta} \right] \frac{J_1(s) e^{-\sqrt{s(s-\lambda\beta)}|y|}}{\sqrt{s(s-\lambda\beta)}} \right. \\
& - \left. \left[\frac{v_0 s}{\lambda\beta} + \frac{1}{2} \frac{A_0}{s} + \frac{B_0}{2\lambda\beta} \right] \frac{J_1(s) e^{-\sqrt{s(s+\lambda\beta)}|y|}}{\sqrt{s(s+\lambda\beta)}} \right. \\
& \left. + \dots \right\} \cos xs ds
\end{aligned} \tag{24}$$

where

$$\begin{aligned}
A_0 = & -\frac{n_0}{\sqrt{EhD}} \frac{\lambda^2}{32v_0(4-v_0)} \left\{ \frac{42-37v_0}{3} + (12-10v_0) \left(\gamma + \ell n \frac{\lambda}{8} \right) \right\} \\
& - \frac{m_0}{v_0(4-v_0)} \left\{ 1 + \frac{12v_0-5v_0^2-8}{4v_0(4-v_0)} \cdot \frac{\pi\lambda^2}{16} \right\} + O(\lambda^4 \ell n \lambda)
\end{aligned} \tag{25}$$

$$\begin{aligned}
B_0 = & \frac{n_0}{i\sqrt{EhD}} \left\{ 1 + \frac{\pi\lambda^2}{16} \left[\frac{5}{4} + \frac{12v_0-5v_0^2-8}{4v_0(4-v_0)} \right] + \frac{\lambda^2\beta^2}{32v_0(4-v_0)} \left[\frac{7v_0^2}{3} \right. \right. \\
& \left. \left. + (10v_0^2-14v_0) + 4\pi i + (10v_0^2-18v_0) \left(\gamma + \ell n \frac{\lambda\alpha}{8} \right) + 6v_0 \left(\gamma + \ell n \frac{\lambda\beta}{8} \right) \right] \right\} \\
& + \frac{m_0}{v_0(4-v_0)} \left\{ v_0 + v_0 \frac{\pi\lambda^2}{16} \left[\frac{5}{4} + \frac{12v_0-5v_0^2-8}{4v_0(4-v_0)} \right] + \frac{\lambda^2\alpha^2}{16} \left[\frac{37v_0-42}{6} \right. \right. \\
& \left. \left. + 5v_0 \left(\gamma + \ell n \frac{\lambda\alpha}{8} \right) - 6 \left(\gamma + \ell n \frac{\lambda}{8} \right) \right] \right\} + O(\lambda^4 \ell n \lambda)
\end{aligned} \tag{26}$$

having used $\gamma = 0.5768\dots = \text{Euler's constant}$. Furthermore, it may be shown, that this series form solution converges to the exact solution for small values of the parameter λ .

STRESS DISTRIBUTION NEAR THE CRACK POINT

The bending and extensional stress components are defined in terms of the displacement function W and stress function F as:

$$\sigma_{x_b} = - \frac{Ez}{(1-\nu^2)c} \left[\frac{\partial^2 W}{\partial x^2} + \nu \frac{\partial^2 W}{\partial y^2} \right] \quad (27)$$

$$\sigma_{y_b} = - \frac{Ez}{(1-\nu^2)c} \left[\frac{\partial^2 W}{\partial y^2} + \nu \frac{\partial^2 W}{\partial x^2} \right] \quad (28)$$

$$\tau_{xy_b} = \frac{2Gz}{c} \frac{\partial^2 W}{\partial x \partial y} \quad (29)$$

$$\sigma_{x_e} = \frac{1}{hc^2} \frac{\partial^2 F}{\partial y^2} \quad (30)$$

$$\sigma_{y_e} = \frac{1}{hc^2} \frac{\partial^2 F}{\partial x^2} \quad (31)$$

$$\tau_{xy_e} = \frac{1}{hc^2} \frac{\partial^2 F}{\partial x \partial y} \quad (32)$$

where z is the dimensionless distance through the thickness h of the shell, measured from the middle surface. Then in view of eqns 23 and 24, the stresses can be expressed in an integral form. When evaluated, these give the following results, where $\epsilon e^{i\theta} = x - 1 + iy$:

Bending Stresses: On the surface $z = h/2c$

$$\sigma_{x_b} = \frac{P_b}{\sqrt{2\epsilon}} \left(- \frac{3-3\nu}{4} \cos \frac{\theta}{2} - \frac{1-\nu}{4} \cos \frac{5\theta}{2} \right) + O(\epsilon^0) \quad (33)$$

$$\sigma_{y_b} = \frac{P_b}{\sqrt{2\epsilon}} \left(\frac{11+5\nu}{4} \cos \frac{\theta}{2} + \frac{1-\nu}{4} \cos \frac{5\theta}{2} \right) + O(\epsilon^0) \quad (34)$$

$$\tau_{xy_b} = \frac{P_b}{\sqrt{2\epsilon}} \left(- \frac{7+\nu}{4} \sin \frac{\theta}{2} - \frac{1-\nu}{4} \sin \frac{5\theta}{2} \right) + O(\epsilon^0) \quad (35)$$

where

$$P_b = \frac{3 n_o \lambda^2}{16(3+\nu)\sqrt{12(1-\nu^2)}hc^2} \left[\frac{5+37\nu}{3} + 2(1+5\nu)(\gamma + \ln \lambda/8) \right] \\ + \frac{6 m_o D}{(3+\nu)h^2c^2} \left[1 - \frac{1+2\nu+5\nu^2}{4(3+\nu)(1-\nu)} \frac{\pi\lambda^2}{16} \right] + O(\lambda^4 \ln \lambda) \quad (36)$$

Similarly we find through the thickness

Extensional Stresses:

$$\sigma_{x_e} = \frac{P_e}{\sqrt{2\epsilon}} \left(\frac{3}{4} \cos \frac{\theta}{2} + \frac{1}{4} \cos \frac{5\theta}{2} \right) + O(\epsilon^0) \quad (37)$$

$$\sigma_{y_e} = \frac{P_e}{\sqrt{2\epsilon}} \left(\frac{5}{4} \cos \frac{\theta}{2} - \frac{1}{4} \cos \frac{5\theta}{2} \right) + O(\epsilon^0) \quad (38)$$

$$\tau_{xy_e} = \frac{P_e}{\sqrt{2\epsilon}} \left(\frac{1}{4} \sin \frac{\theta}{2} - \frac{1}{4} \sin \frac{5\theta}{2} \right) + O(\epsilon^0) \quad (39)$$

where

$$P_e = \frac{n_o}{hc^2} \left[1 + \frac{5\pi\lambda^2}{64} \right] + \frac{\sqrt{12(1-\nu^2)} m_o D \lambda^2}{32(3+\nu)(1-\nu)h^2c^2} \left[\frac{5+37\nu}{3} + 2(1+5\nu)(\gamma + \ln \lambda/8) \right] + O(\lambda^4 \ln \lambda) \quad (40)$$

As a result of the Kirchhoff boundary condition, the bending shear stress τ_{xy_b} does not vanish in the free edge. For the flat sheet this difficulty was discussed by Knowles and Wang who considered Reissner bending⁽⁵⁾. Furthermore, it is apparent from the above equations that there exists an interaction between bending and stretching, except that in the limit as $\lambda \rightarrow 0$ the stresses of a flat sheet are recovered and coincide with those obtained previously for bending⁽⁶⁾ and extension⁽⁷⁾. We are thus in a position to correlate, at least locally, flat sheet behavior with that of initially curved specimens.

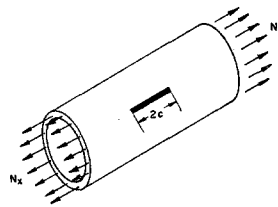


Figure 2. Cracked Shell under Uniform Axial Extension N_x and Internal Pressure q_o

As a practical matter, consider a shell subjected to a uniform internal pressure q_o with an axial extension $N_x = \frac{q_o R}{2}$, $M_y = 0$ far away from the crack (see Figure 2). The stresses along the line of crack prolongation are found for $\nu = 1/3$ and $\lambda = 0.98$ to be:

$$\sigma_{y_{total}}(\epsilon, 0) \approx \frac{0.79}{\sqrt{\epsilon}} q_o R/h \quad (41)$$

$$\sigma_{x \text{ total}}(\epsilon, 0) \approx \frac{0.97}{\sqrt{\epsilon}} q_0 R/h \tag{42}$$

where, based on the Kirchhoff theory, the stresses σ_x and σ_y have the same sign but differ in magnitude. This difference is due to the fact that in a cylindrical shell the curvature varies between zero and a constant as one considers different angular positions with respect to the line of the crack. On the other hand, for a spherical shell⁽²⁾ and for a flat plate⁽⁶⁾, for which the curvature remains constant in all directions, we obtain a "hydrostatic tension" stress field.

FRACTURE CRITERION

In precisely the same manner used for a fracture criterion for a spherical cap, we derive the following approximate criterion for a cylindrical panel, at $\nu = 1/3$ and the Griffith stress $\sigma^* = (16G\gamma^*/\pi c)^{1/2}$:

$$(1 + 0.49 \lambda^2) (\bar{\sigma}_e/\sigma^*)^2 + 0.21 (1 - 0.10 \lambda^2) (\bar{\sigma}_b/\sigma^*)^2 - (0.04 - 0.10 \ln \lambda) \lambda^2 (\bar{\sigma}_e/\sigma^*) (\bar{\sigma}_b/\sigma^*) + O(\lambda^4 \ln \lambda) = 1 \tag{43}$$

where the barred quantities denote applied stress. This equation represents a family of ellipses which are plotted in Figure 3. Note that the curves

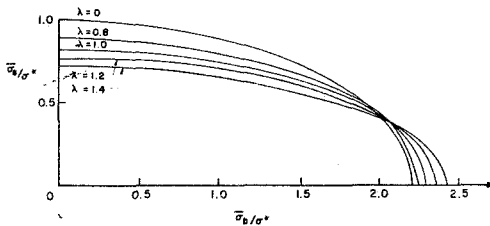


Figure 3. Extension-Bending Interaction Curves for a Cylindrical Shell Containing a Crack, for $\nu = 1/3$;

$$\lambda = \sqrt[4]{12(1 - \nu^2)} c/\sqrt{Rh}$$

cross each other, which did not occur in the case of a spherical shell (see Figure 4). The author conjectures that this is due to the slower rate of convergence of the former case and that, when higher orders of λ are used in the solution, the curves will correct themselves to give the same trend.

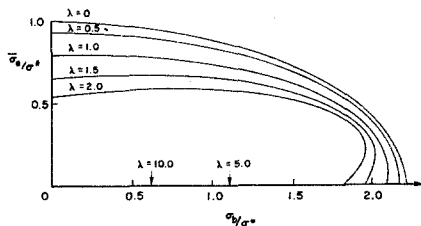


Figure 4. Extension-Bending Interaction Curves for a Shallow Spherical Shell Containing a Crack, for $\nu = 1/3$;

$$\lambda = \sqrt[4]{12(1 - \nu^2)} c/\sqrt{Rh}$$

For the special case $\bar{\sigma}_b = 0$ eqn 43 reduces to:

$$(1 + 0.49 \lambda^2) (\bar{\sigma}_e/\sigma^*)^2 + O(\lambda^4 \ln \lambda) = 1 \tag{44}$$

Specializing further to a cracked shell under uniform axial extension $N_x = q_0 R/2$ and internal pressure q_0

$$\left(\frac{q_0 R/h}{\sigma^*}\right)^2 \approx 1 - 0.49 \lambda^2 \tag{45}$$

which gives the maximum internal pressure that the shell may withstand before fracture. A plot of eqn 45 is given in Figure 5. Similar results were obtained experimentally by Sechler and Williams⁽³⁾ for pressurized monocoque cylinders.

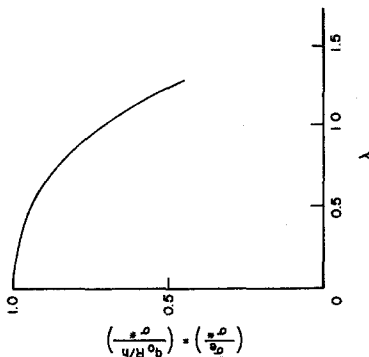


Figure 5. Critical (Fracture) Pressure in a Cylindrical Shell, for $\nu = 1/3$; $\lambda = \sqrt[4]{12(1 - \nu^2)} \frac{c}{\sqrt{Rh}}$

CONCLUSIONS

- As in the case of a spherical shell,
- (i) the stresses are proportional to $1/\sqrt{\epsilon}$
- (ii) the stresses have the same angular distribution as that of a flat plate
- (iii) an interaction occurs between bending and stretching
- (iv) the stress intensity factors are functions of R ;
in the limit as $R \rightarrow \infty$ we recover the flat plate expressions. Thus we may write

$$\frac{\sigma_{shell}}{\sigma_{plate}} \approx 1 + (a + b \ln \frac{c}{\sqrt{Rh}}) \frac{c^2}{Rh} + O\left(\frac{1}{R^2}\right) \tag{46}$$

where the expression in parentheses is a positive quantity. From this and the corresponding result for a spherical cap, it would appear that the general effect of initial curvature is to increase the stress in the neighborhood of the crack point. It is also of some practical value to be able to correlate flat sheet behavior with that of initially curved specimens. In experimental work on brittle fracture for example, considerable effort might be saved since, by eqn 46, we would expect to predict the behavior of curved sheets from flat sheet tests.

In conclusion it must be emphasized that the classical bending theory has been used in deducing the foregoing results. Hence only the Kirchhoff shear condition is satisfied along the crack, and not the vanishing of both individual shearing stresses. While outside the local region the stress distribution should be accurate, one might expect the same type of discrepancy to exist near the crack joint as that found by Knowles and Wang in comparing Kirchhoff and Reissner bending results for the flat plate case. In this case the order of the stress singularity remained unchanged but the circumferential distribution around the crack changed so as to be precisely

the same as that due to solely extensional loading. Pending further investigation of this effect for initially curved plates, one is tempted to conjecture that the bending amplitude and angular distribution would be the same as that of stretching.

ACKNOWLEDGMENT

This work was supported in part by the USAF Aerospace Research Laboratories, Office of Aerospace Research. The author thanks J. L. Swedlow for help in preparation of the manuscript.

Received February 23, 1965.

REFERENCES

1. E. S. Folias International Journal of Fracture Mechanics, 1, 1, March 1965, pp.20-46.
See also ARL 64-23, Aerospace Research Laboratories, Office of Aerospace Research, U.S. Air Force, January 1964.
2. E. E. Sechler and "The Critical Crack Length in Pressurized, Monocoque Cylinders." Final Report on
M. L. Williams Contract NAW-6525, California Institute of Technology, September 1959.
See also; M. L. Williams, Proceedings of the Crack Propagation Symposium, 1, College
of Aeronautics, Cranfield (England), September 1961, pp.130-165.
3. E. S. Folias ARL 64-174, Aerospace Research Laboratories, Office of Aerospace Research, U.S.
Air Force, October 1964.
4. K. Marguerre Proceedings of Fifth Congress of Applied Mechanics, 1938, pp.93-101.
5. J. K. Knowles and Journal of Mathematics and Physics, 39, 1960, pp.223-236.
N. M. Wang
6. M. L. Williams Journal of Applied Mechanics, 28, March 1961, pp.78-82.
7. M. L. Williams Journal of Applied Mechanics, 24, March 1957, pp.109-114.

RÉSUMÉ - A la suite d'une analyse antérieure d'une fissure dans une coquille sphérique, on a présenté les contraintes dans une coque cylindrique contenant une fente axiale. Le comportement singulier de l'inverse de la racine carrée des contraintes particulières aux problèmes de rupture, est obtenu en même temps selon les composantes d'extension et de flexion. Cette singularité peut-être rapprochée de celle trouvée dans une plaque initialement plate, à l'aide de:

$$\frac{\sigma_{\text{coque}}}{\sigma_{\text{plaque}}} \approx 1 + (a + b \ln \frac{c}{\nu Rh}) \frac{c^2}{Rh} + \dots$$

où la quantité entre parenthèses est positive. On a déduit un critère de rupture, basé sur la théorie de Griffith, et on a présenté les courbes d'interaction entre flexion et tension.

ZUSAMMENFASSUNG - In Fortsetzung der fruheren Analyse eines geradlinigen Risses in einer kugelfoermigen Kappe werden jetzt die Spannungen in einer Zylinderschale, die einen Riss in axialer Richtung aufweist, gegeben. Die diesen Problemen eigene Singularitaet der Spannungen, die umgekehrt proportional der Wurzel aus der Entfernung von der Riss-spitze sind, wird auch hier fuer die Zug- und Biegekomponenten erhalten. Diese Singularitaet kann zu derjenigen, die in einer urspruenglich ebenen Platte gefunden wird, in folgenden Zusammenhang gebracht werden

$$\frac{\sigma_{\text{Schale}}}{\sigma_{\text{platte}}} \approx 1 + (a + b \ln \frac{c}{\nu Rh}) \frac{c^2}{Rh} + \dots$$

Wobei die Groesse in Klammern positive ist. Ein angenaehertes Bruchkriterium, das auf Griffith's Theorie beruht, ist abgeleitet worden und Biegungs-Zug Wechselwirkungskurven sind fuer diesen Fall bestimmt worden.